Channeling of electrons in a crossed laser field

S. B. Dabagov,[1,2,3,*] A. V. Dik,[2] and E. N. Frolov[2,4]

[1]*INFN Laboratori Nazionali di Frascati, Frascati (Roma), 00044, Italy*
[2]*RAS P.N. Lebedev Physical Institute, Moscow, 119991, Russia*
[3]*National Research Nuclear University MEPhI, Moscow, 115409, Russia*
[4]*National Research Tomsk Polytechnic University, Tomsk, 634050, Russia*

In this article a new analytical description of the effective interaction potential for a charged particle with the field of two interfering laser beams is presented. The potential dependence on the lasers intensities, orientation and parameters of the particle entering the considered system is analyzed. For the first time the phenomenon of effective potential inversion (or "*relativistic reversal*") is described for arbitrary lasers crossing angle. Threshold electron velocity values for the phenomenon are introduced and its extended illustration based on numerical simulations for two laser beams polarizations is presented. In addition the projectile radiation spectral distribution is given and general estimations on the expected beam radiation yield are outlined.

I. INTRODUCTION

The topic of electrons dynamics in crossed laser beams is gaining growing attention. Usually the case of standing electromagnetic wave being the result of two counter-propagating laser beams is considered. Kapitza and Dirac were the first who referred to electrons dynamics in such an interference field in a well-known paper [1] introducing Kapitza-Dirac phenomenon. They have described for the first time the possibility of electron beam diffraction in standing optical field.

Many papers were published lately proposing a tool for electron beam size monitor [2], new-type free electron laser with optical undulator [3–7], channeling radiation source [8–10] (all being based on electrons dynamics in the field of two laser beams) and works clarifying processes in such a system [11–13]. In this work the electron motion in optical lattice formed by crossed linearly polarized laser beams, in plane electromagnetic waves approximation, is described in terms of particles channeling.

A. Channeling phenomenon

Usually channeling phenomenon is related to the beam propagation in aligned crystals. As known, the beam channeling in crystals takes place during relativistic charged particles motion in periodic structures of the crystals close to the main crystallographic directions that form the crystal axes or planes. For relativistic electron traveling almost parallel to that direction, the potential of interaction between the electron and a set of the lattice atoms (ions) could be averaged along the propagation direction. Potential well formed in such a way can limit transverse motion of the projectile within well-defined channels, i.e., the relativistic particle becomes undulating in transverse plane at fast longitudinal motion down to the channel [14,15]. For more than 50 years of intense studies the basics of crystal channeling for charged beams have been defined in detail and described in many scientific papers and books, discussed in a number of conferences and workshops. Presently crystal channeling is known as a useful technique for beam steering, while the related phenomena to crystal channeling are promising candidates for coherent radiation sources (for details, see in [16]). Moreover, the phenomenology of beams channeling becomes very useful for describing neutral beams handling with help of various beam guiding structures [17,18]. Besides, channeling conditions could be realized for particles not only in medium (crystals, capillaries [17,18] and nanotubes [19–21], plasma [22–25]) but also in high intensity electromagnetic fields of specific configurations [26] that is the scope of this article. Generally saying, channeling phenomenology may be applied for any kind of charged or neutral particle beams motion in the external fields defined by long transversely limited channels. And various features of the structure as a periodic structure, for instance, may supply additional peculiarities of beam passing through such structures.

B. Ponderomotive potential

In the region of two laser beams overlapping the ponderomotive force characterized by averaged effective potential affects charged particles. The ponderomotive

potential forms planar (one-dimensional) potential wells. It was shown that a charged particle can be trapped in such a well and oscillate in it. The typically used ponderomotive force expression [27,28] is written in the following way

$$\mathbf{F}_p = \frac{e^2}{4\omega_0^2 m} \vec{\nabla}|\mathbf{E}(x)|^2, \tag{1}$$

where $e = |e|$ and m are, correspondingly, the charge and mass of the electron, ω_0 is the laser frequency and $\mathbf{E}(x)$ is the electrical field amplitude distribution over x-coordinate.

Lately Kaplan et al. have pointed out that the ponderomotive force expression is much more complex [11,12]. This force depends not only on lasers intensities but also on their polarization and energy of the particle. One of the most interesting results in their work is ponderomotive potential inversion description. In brief, if the longitudinal (parallel to the channels axes) speed of a charged particle placed in the field of two counterpropagating laser beams equals some defined critical value then the particle feels no periodic ponderomotive potential at all, if the beams are p-polarized. In other words, the height of one-dimensional potential channels borders becomes zero. And if the particle speed is greater then the critical value, ponderomotive potential sign inversion is observed. That means, attracting potential regions become scattering ones and vice versa. Apart of this peculiarity, the motion of a charged particle in the presence of two counterpropagating laser beams could be described as a sum of slow averaged motion in the effective ponderomotive potential and simultaneously rapid small oscillations defined by the lasers frequency. Such motion is treated by different authors as betatron oscillations [29], FEL oscillations [3–7], channeling oscillations [3,8,9,30,31] or simply called averaged (slow) oscillations [1,11–13]. We here shortly outline why channeling analogy is chosen by us.

C. Optical lattice channeling

As known, there is much in common between particles dynamics in crossed laser beams and processes found in FEL undulators, betatron oscillations in plasma channels and crystal channeling. We should give a short remark on why the channeling point of view could be the most appropriate for considering the phenomenon.

First of all, interference of two crossed laser beams creates electromagnetic field peaks and nodes, i.e., optical lattice, which is similar to the crystal lattice. This creates a semblance of crystal lattice in the absence of actual medium. Furthermore, averaging interaction of a particle with both crystal and optical lattices one derives effective potential responsible for particle channeling in these systems. And this descriptive similarity is not the only reason for treating the considered process as channeling.

Another reason lies in the similarity of possible applications and effects found in optical lattice and in crystal channeling. As shown in [3,8–10,30] and described below, the effective potential of both crystal and optical lattices could be very similar and both are capable of trapping electrons, so that channeled electron beams may be transported, focused and reflected by potential of both lattices. Bending a crystal one obtains a tool for charged particles beams steering [32] and bent laser channels may be also applied for this. Such channels may be formed by illuminating a curved reflecting surface with a laser at some angle that creates an interference region with potential channels near the surface. The peculiarities of beam channeling in a bent laser field will be described in a separate work.

Besides, recently various researches have shown different regimes of charged particles dynamics in the presence of intense laser fields that are analogous to crystal volume reflection, to both planar [8–10,26,30,33] and axial [9] crystal channeling and optical undulating.

II. ELECTRONS IN CROSSED LASER FIELD

The results below were derived for a relativistic electron in the field of crossed p-polarized laser beams using plane wave approximation. The averaged field in such a system is characterized by the planes of equal potential forming planar channels. We show here channels parameters dependence on the lasers crossing angle.

A. Interaction potential

Let us consider two crossed laser beams of the ω_0 frequency with the wave vectors $\mathbf{k}_1$ and $\mathbf{k}_2$, which lie in the xOz plane at the acute angles η with respect to the Oz direction (see Fig. 1). Let the electron move in the combined laser filed, which is situated in the region where two laser beams form a standing wave structure. Using plane wave approximation, the electromagnetic field in some region of beams overlapping could be described by a set of equations
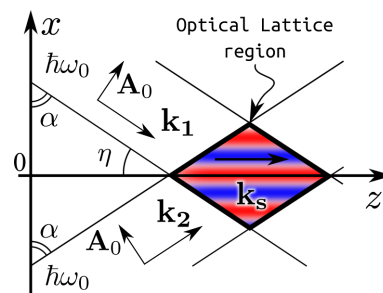
FIG. 1. The general scheme of the considered system. The effective potential channels (shown in color) axes are parallel to $0z$-axis.

$$\begin{Bmatrix} \varphi \\ A_x \\ A_y \\ A_z \end{Bmatrix} = \begin{Bmatrix} 0 \\ -2A_0 \sin\alpha \cos(k_x x) \cos(\omega_0 t - k_z z) \\ 0 \\ 2A_0 \cos\alpha \sin(k_x x) \sin(\omega_0 t - k_z z) \end{Bmatrix}, \quad (2)$$

where $k_{x,z}$ are the absolute values of appropriate $\mathbf{k}_{1,2}$ components, and A_0 is the longitudinal vector potential amplitude.

This structure is similar in some way to the crystal lattice, seen by a high-velocity projectile, that is a set of crystal nodes, forming crystallographic planes and axes. The standing waves can be represented as the effective potential wells, the channels, periodically situated in a transverse plane that can trap the electron at specific conditions. The nonrelativistic electron trajectory can be classically derived with the help of the well-known Kapitza formalism [34], within which the trajectory of a channeled electron could be presented as a sum of slow channeling oscillations and rapid small amplitude oscillations. Such approach allows one to write down the analytical expression for channeled electron trajectory in the case of small channeling oscillations near the channel bottom. For the case of large amplitude channeling oscillations the motion equation cannot be linearized. Thus, only qualitative estimations and computer simulations are feasible.

B. Effective potential for relativistic electron

It should be underlined that to use the Kapitza method becomes impossible directly for relativistic electrons since their speed is comparable with the speed of light. However, one may go to new variables, using generating function S

$$S = (z - v_0 t)P'_z; \qquad \mathbf{x}'_\perp = \mathbf{x}_\perp; \qquad \mathbf{P}'_\perp = \mathbf{P}_\perp;$$
$$z' = z - v_0 t. \qquad (3)$$

Here v_0 is the electron initial longitudinal speed ($v_0 \to c$), electron position is described with $\mathbf{x} = (\mathbf{x}_\perp, z) = (x, y, z)$ and electron generalized momentum is $\mathbf{P} = (\mathbf{P}_\perp, P_z)$. Thus, for the electron in the field characterized by the vector-potential $\mathbf{A}$ the motion equations are

$$\dot{p}'_i = -\frac{e}{c} \left[\frac{\partial A_i}{\partial t} - v_0 \frac{\partial A_z}{\partial x_i'} + \dot{x}'_j \left(\frac{\partial A_i}{\partial x_j'} - \frac{\partial A_j}{\partial x_i'} \right) \right] \quad (4)$$

$$\dot{x}'_i = \frac{c p'_i}{\sqrt{(mc)^2 + p'_j p'_j}} - v_0 \delta_{iz}, \quad (5)$$

where p'_i is the kinematic momentum, δ_{ij} is the delta Kronecker symbol. These equations could be solved within the Kapitza method, i.e., the electron trajectory as mentioned above may be expressed as a sum of slow and rapid oscillations $x'_i = \bar{x}_i + \xi_i$. The same is true for electron

momentum $p'_i = \bar{p}_i + p^\xi_i$. The right-hand side of Eq. (4) then may be written in the following way $F_i(\mathbf{x}', v_0, t) + \dot{x}'_j B_i^j(\mathbf{x}', t)$, thus—taking into account that $|\dot{\mathbf{x}}'/c| \ll 1; p'_z \gg |\mathbf{p}_\perp|'$—the motion equations are split for slow oscillations

$$\begin{cases} \dot{\bar{p}}_i = \overline{\xi_j \frac{\partial F_i(\bar{\mathbf{x}}, v_0, t)}{\partial \bar{x}_j}} + \overline{\dot{\xi}_j B_i^j(\bar{\mathbf{x}}, t)}, \\ \bar{\mathbf{p}}_i = \bar{\gamma} m \dot{\bar{x}}_i, \end{cases} \quad (6)$$

and rapid oscillations

$$\begin{cases} \dot{p}^\xi_i = F_i(\bar{\mathbf{x}}, v_0, t), \\ p^\xi_z = \bar{\gamma}^3 m \dot{\xi}_z; \quad \mathbf{p}^\xi_\perp = \bar{\gamma} m \dot{\xi}_\perp \mathbf{e}_\perp, \end{cases} \quad (7)$$

where $\bar{\gamma} = \sqrt{1 + (\bar{p}_z/mc)^2}$. The averaged longitudinal momentum in the system is constant

$$\bar{p}_z = \frac{m v_0}{\sqrt{1 - \beta_\parallel^2}}. \quad (8)$$

Averaging by rapid oscillations one derives the effective potential expression

$$U_{\text{eff}} = -U_{\text{am}} \cos(2kx \cos\alpha), \quad (9)$$

$$U_{\text{am}} = \frac{e^2 A_0^2 ((1 + \cos^2\alpha)\beta_\parallel^2 - \cos(2\alpha) - 2\beta_\parallel \sin\alpha)}{2\gamma_\parallel mc^2 (1 - \beta_\parallel \sin\alpha)^2}, \quad (10)$$

where $\beta_\parallel = v_0/c$ and positive $\beta_\parallel$ means that the electron moves in the direction of $\mathbf{k}_s = \mathbf{k}_1 + \mathbf{k}_2$, while negative $\beta_\parallel$—in opposite direction.

In the case of *equal circular lasers polarization* (for both lasers it is either right-handed or left-handed) in the same beams geometry the use of the described method yields in the following effective potential amplitude expression

$$U_{\text{am}}^c = \frac{e^2 A_0^2 (1 + 2\beta_\parallel^2 - \cos(2\alpha) - 4\beta_\parallel \sin\alpha)}{2\gamma_\parallel mc^2 (1 - \beta_\parallel \sin\alpha)^2}. \quad (11)$$

The method is applicable to the system only when both rapid momentum and trajectory oscillations are considerably less than the slow ones: $\xi_i \ll \bar{x}_i$ and $p^\xi_i \ll \bar{p}_i$. Notably, the effective potential does not depend on the external field frequency. And introducing phase difference for the electromagnetic waves only shifts the potential spatially in the transverse direction but does not change channel height or width.

In general, the particle motion in the potential (9) is expressed via the elliptic integral. And in the case of averaged oscillations close to the channel axis the motion equations could be linearized. Hence, the trajectory is

characterized by $\Omega_1 = 2k\cos\alpha\sqrt{U_{am}/(\gamma_\parallel m)}$ frequency for channeling oscillations (within standing wave structure) and $\Omega_2 = \omega_0(1 - \beta_\parallel \sin\alpha)$ frequency for rapid oscillations due to the particle interaction with the interference laser field. This motion representation is used below for the particle radiation calculation.

C. Potential inversion

The above derived expressions (9) and (10) describe the effective potential in the region of two p-polarized laser beams crossed at arbitrary angle. For $\alpha = 0$ the beams are counterpropagating and the geometry is similar to that considered in [11–13]. The potential amplitude in this case is positive for $|\beta_\parallel| > 1/\sqrt{2}$ and negative otherwise. This corresponds to the results reported in [11–13] and means that for an electron moving at the speed $|\beta_\parallel| = 1/\sqrt{2} = -\beta_1^{inv} = \beta_2^{inv}$ no periodic potential is formed. Let us call these two values the "*inversion speed*" $\beta_{1,2}^{inv}$. And β^{min} is the electron speed value for which at chosen α the value of $U_{am}\gamma_\parallel$ becomes minimal. When the electron speed is $|\beta_\parallel| > 1/\sqrt{2}$, the regions of interference electric field peaks are scattering for it. And for $|\beta_\parallel| < 1/\sqrt{2}$ these regions become attracting. This potential inversion is observed only for p-polarized crossed laser beams.

The expressions (9) and (10) cover arbitrary lasers crossing angles and the analysis of Eq. (10) shows that the values of inversion speed may be expressed by

$$\beta_{1,2}^{inv}(\alpha) = \frac{\sin\alpha \mp \sqrt{2}\cos^2\alpha}{1 + \cos^2\alpha}. \qquad (12)$$

This function is presented in Fig. 2(a). One can see that $|\beta_1^{inv}| = |\beta_2^{inv}|$ only for $\alpha = 0$. Varying α causes shift of the $[\beta_1^{inv}, \beta_2^{inv}]$ range to positive $\beta_\parallel$ region [see Fig. 2(b)]. This means that an electron with $\beta_\parallel = 0.978$ in the region of two laser beams overlapping at the angle of 10° ($\alpha = 85°$) is affected by no ponderomotive force ($U_{am}\gamma_\parallel = 0$), whereas an electron with $\beta_\parallel = 0.9962$ could become channeled in the effective potential ($U_{am}\gamma_\parallel = -1$).

For the chosen electron longitudinal energy values of lasers crossing angle $\alpha = \alpha^{min}$, for which $U_{am}\gamma_\parallel(\alpha^{min}, \beta_\parallel) = -1$, could be easily derived from the expression (10)

$$\sin\alpha^{min} = \beta_\parallel. \qquad (13)$$

Such electron in the field of two lasers crossed at the angle of α^{min} oscillates near the transverse electric field peaks. On the other hand, channeled electron with $\beta_\parallel < \beta_1^{inv}$ (or $\beta_\parallel > \beta_2^{inv}$) oscillates near the transverse electric field nodes plane.

In Fig. 3 the projections of phase space trajectories onto the plane of transverse momentum and coordinate are
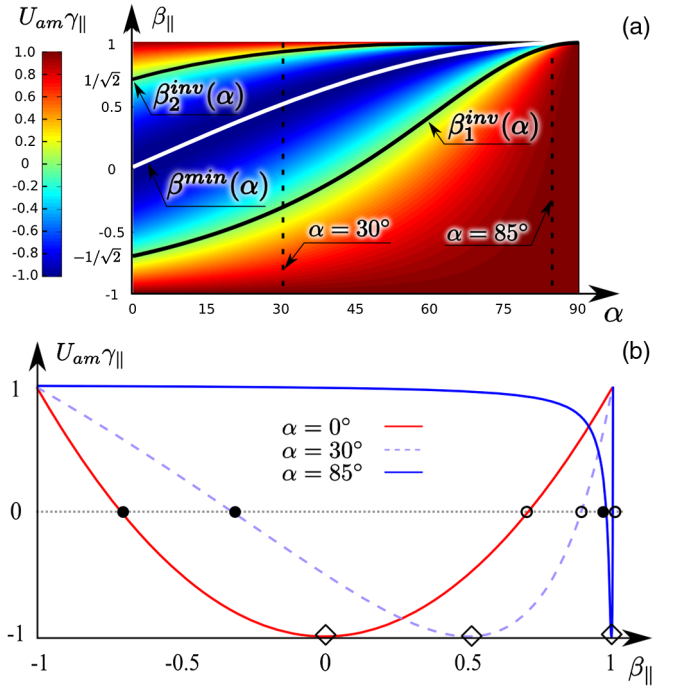
FIG. 2. (a) The averaged potential amplitudes normalized by $(e^2A_0^2)/(2\gamma_\parallel mc^2)$ as a function of $\beta_\parallel$ and α is shown in color. Inversion speed values $\beta_{1,2}^{inv}$ as a functions of α are shown in black. And $\beta^{min}(\alpha)$ is shown in white. (b) Normalized potential amplitudes for two p-polarized laser beams, crossed at different angles. The inversion speed values β_1^{inv} are marked with closed circle, values of β_2^{inv}—with open circle, and β^{min}—with diamond for each α.

presented for both channeled and over-barrier electrons in the field of laser beams crossed at the angle of 30° ($\alpha = 75°$). The inner closed curves (in blue) correspond to channeled electrons with transverse energies less than potential well height. Over-barrier electrons (in red) are characterized by transverse energies greater than the barrier height and not limited within the channels.

For electron with $\beta_\parallel = \beta^{min}$ the channel borders are situated at $x/d_{ch} = 0.5 + n$ and, correspondingly, the channel centers—at $x/d_{ch} = n$ [see Fig. 3(a)]. On the contrary, electron with longitudinal velocity $\beta_\parallel \to 1 > \beta_2^{inv}$ could be trapped by the channels, central axes of which are placed at $x/d_{ch} = 0.5 + n$ [see Fig. 3(b)], where $n = 0, \pm 1, \pm 2, \ldots$

Notably, the effective potential $U_{am}^c\gamma_\parallel$ for the case of equal circular lasers polarization normalized to unity has the form exactly similar to Eq. (10) but its minimal value is zero (see Fig. 4). This case for $\alpha = 0$ was considered in [11–13] previously, providing the same results. But the expression (11) describes the potential amplitude for arbitrary α showing that an electron in the field of circularly polarized lasers crossed at the angle of $\alpha^{min} = \arcsin\beta_\parallel$ feels no effective potential, and no inversion is observed for circularly polarized laser beams. This is the main difference comparing to the p-polarization case.
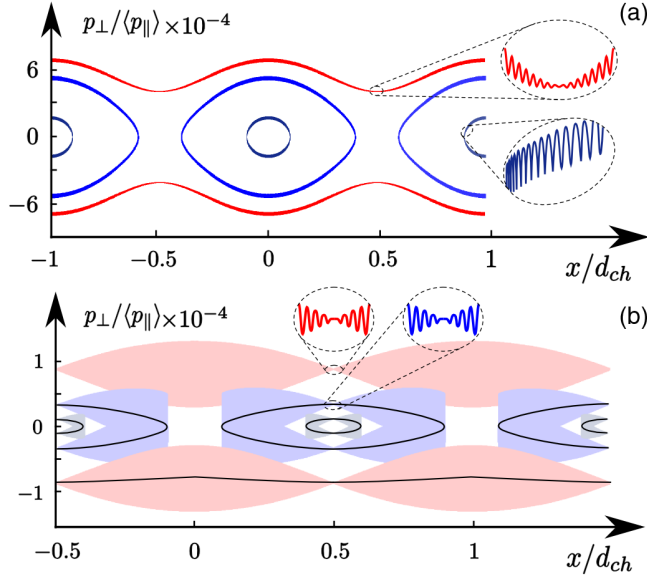
FIG. 3.   Numerically calculated transverse phase-space trajectories for electron with $\beta_\parallel = \beta^{\min}$ (a) and $\beta_\parallel = 0.99986$ (b) moving in a channel formed by two p-polarized lasers of $\lambda = 800$ nm wavelength and 5 TW/cm^2 intensity for each one. The electron transverse momentum is normalized by the averaged longitudinal momentum, while the transverse coordinates by the channel width $d_{\rm ch} \equiv \lambda_0/(2\sin\eta)$. Channeled (under-barrier) trajectories are shown in blue, while quasichanneled (over-barrier) in red. The rapid oscillations could not be properly visualized and are outlined near the plots. The averaged phase-space trajectories are also demonstrated in solid black lines. To build these trajectories the 4th order Runge-Kutta method was used for the electrons motion equations integration.

For details, in the supplemental materials [35] one can find two animations of channeled electron dynamics numerical simulations. These results were received by motion equations integration for the electron in the field of p-polarized and circularly polarized electromagnetic waves. The 4th order Runge-Kutta method was used. The projectile longitudinal velocity varies from $\beta_\parallel = -0.969$ to $\beta_\parallel = 0.999$ just as if the additional longitudinal electric field was imposed on the region. Current electron longitudinal speed is shown in the upper region of the video. Spatial distribution of the normalized potential distribution $U_{\rm am}\gamma_\parallel(x/d_{\rm ch})$ is shown for every moment of time in the right region of the video. In the main area averaged transverse oscillations of the electron is put onto the current potential distribution presented in color.

III. CHANNELED ELECTRONS RADIATION

Obviously, the possibility of charged beam channeling in electromagnetic lattices becomes rather interesting due to the ability of beams shaping by means of tools based on this process. Moreover, speaking on possible applications of the interaction under consideration one should outline that it
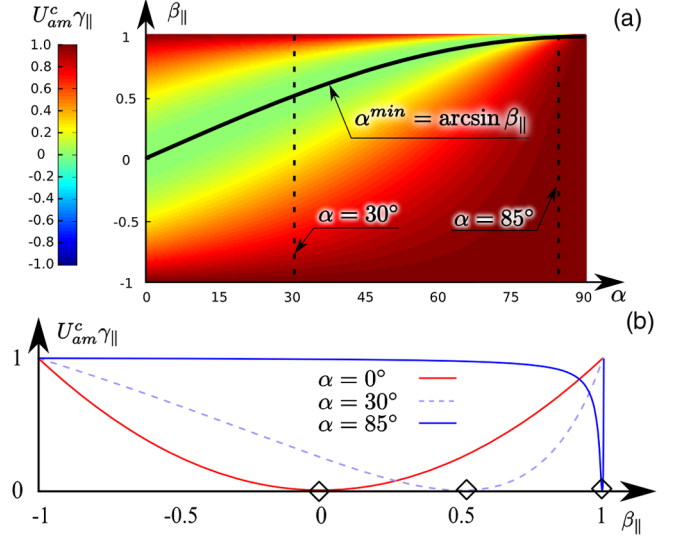
FIG. 4.   (a) Normalized to unity potential amplitude $U_{\rm am}^c\gamma_\parallel$ as a function of $\beta_\parallel$ and α for circularly polarized lasers case is shown. The amplitude of effective potential reaches minimal value equal zero on the curve $\alpha^{\min} = \arcsin\beta_\parallel$. (b) Normalized potential amplitudes for two circularly polarized laser beams, crossed at different angles. The values $\beta^{\min} = \sin\alpha$ are marked with diamond for each α.

can be used as a promising tunable source of intense radiation. The radiation spectrum of a charged particle emitting in a crossed laser field is characterized by two peak frequencies $\omega_1 = \Omega_1/[1 - \beta_\parallel\cos(\theta)]$ and $\omega_2 = \Omega_2/[1 - \beta_\parallel\cos(\theta)]$ [10], where $\Omega_{1,2}$ were defined before. Both of them being measured in the forward direction ($\theta = 0$) are shifted by the factor of $\sim 2\gamma_\parallel^2$ due to the Doppler effect. The first one (ω_1) corresponds to slow channeling electron oscillations in the potential well of a system and does not depend on the laser frequency ω_0. The ω_2 radiation frequency is caused by the electron interaction with the interference laser beams field. Hence, ω_2 is strictly defined by the electron velocity as well as by the wave vectors $\mathbf{k}_1$ and $\mathbf{k}_2$. The intensity of electromagnetic radiation by a laser-channeled electron can be described by the 4-potential $A_\mu = (\mathbf{A}, \varphi)$

$$A_\mu(\mathbf{r}, t) = \frac{4\pi}{c}\int j_\mu(\mathbf{r}', t')G(\mathbf{r} - \mathbf{r}', t - t')d^3r'dt', \quad (14)$$

where $j_\mu = (\mathbf{j}, c\rho)$ is the 4-current, $G(\mathbf{r} - \mathbf{r}', t - t')$ is the Green function. The field can be found in the far-field zone and represented as a sum of spherical monochromatic waves. Taking into account that a relativistic particle emits radiation in a narrow forward directed solid cone, one could define the analytical expression for radiation spectrum of relativistic channeled electron moving near the bottom (center) of the cross-laser channel [10]

$$\frac{dP}{d\omega} = \sum_{i=1}^{2} \frac{e^2 \Omega_i^3 a_i^2 \gamma_\parallel^2}{c^3} \zeta_i (1 - 2\zeta_i + 2\zeta_i^2) \Theta[\pi N_i (1 - \zeta_i)], \tag{15}$$

where ω is the radiation frequency, a_1 is the amplitude of channeling oscillations, and a_2 is the amplitude of rapid oscillations, N_i is the number of Ω_i-frequency particle oscillations, $\zeta_i = \omega/(2\gamma_\parallel^2 \Omega_i)$, and $\Theta(x) = 0.5 + \text{si}(2x)/\pi - \sin^2(x)/\pi x$ [36,37]. Knowing channeling oscillation frequency Ω_1 (presented above) for relativistic electron ($\beta_\parallel \to 1$) in the considered system one can easily derive maximum energy of emitted photons. For $\alpha = 75°$ it is expressed by

$$\hbar\omega_m^{\text{rad}} \approx 7.7 \times 10^{-10} \gamma_\parallel \sqrt{I}, \tag{16}$$

where $\hbar$ is the Planck constant in eVs and I is the external field intensity in W cm^{-2}. It corresponds to Doppler shifted radiation in forward direction. However, when the averaged electron oscillations amplitude is of the same order as channels width d_{ch} Eq. (15) and (16) are not directly applicable. The trajectory in this case becomes nonharmonic, hence several low-frequency radiation peaks emerge.

The numerically calculated spectrum is shown in Fig. 5 (blue curve). It represents radiation of 20 MeV electron oscillating in the field of two plane p-polarized electromagnetic waves of equal intensity $I = 10^{11} \text{ W cm}^{-2}$ crossed at 30° ($\alpha = 75°$). Electron initial transverse speed is zero and initial transverse coordinate is $x_0 = 0.9d_{\text{ch}}$. Therefore its oscillations are nonharmonic and additional peak at $\omega = 26.7$ THz occurs. The main peak at $\omega \approx 9$ THz equals to the main averaged oscillations frequency ($\Omega_1 = 3$ GHz) Doppler shifted by $2\gamma_\parallel^2$. Notably, it is similar
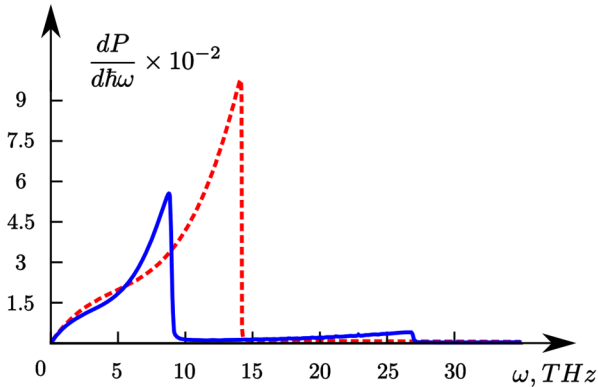
FIG. 5. Photon yield for single electron calculated numerically for $N_1 = 37$ *large amplitude* averaged oscillations (blue curve). For $N_1 \to \infty$ *small amplitude* averaged oscillations the spectrum is characterized by (15) and is presented by the red dashed curve. All the conditions ($I = 10^{11} \text{ W cm}^{-2}$, $\alpha = 75°$ and electron energy 20 MeV) except the initial transverse position for these cases are similar.

to well-known crystal channeling radiation spectra (e.g., see spectra in [10] and [38]).

If the same electron is initially 10 times closer to the channel axis, it performs almost harmonic oscillations with 10 times less amplitude at $\Omega_1 = 4.7$ GHz frequency. Hence, Eqs. (15) and (16) are applicable. The radiation spectrum for this case is calculated analytically and illustrated in Fig. 5 (red curve) for $N_1 \to \infty$.

For the external laser intensities $I \sim 10^{12} \text{ W cm}^{-2}$ the maximum of emitted channeling radiation spectral distribution falls on $\lambda_1 \approx 1 \mu m$ for a channeled electron with $\gamma_\parallel \approx 10^3$. And for $I \sim 10^{20} \text{ W cm}^{-2}$ the electron emits photons with maximum energy of ~ 10 keV. Notably, for strong laser fields no averaged electron motion can be observed. Threshold laser intensity value I_{max} for such case is partly covered in [39] and is not in the scope of the current work. However, we highlight that I_{max} is a function of the electron initial energy, i.e., for an electron with $\gamma_\parallel = 10$ and laser intensity $I \sim 10^{20} \text{ W cm}^{-2}$ no electron channeling is observed. On the other hand, numerical calculations for 500 MeV electron yield channeling oscillations frequency equivalent to the presented Ω_1 value. Therefore, the method and formulas presented above are applicable for the case of $I = 10^{20} \text{ W cm}^{-2}$ and $\gamma_\parallel = 10^3$. The analysis of threshold laser intensity for electron channeling will be published in a separate work.

Total low-frequency power emitted by the channeled electron can be then evaluated by

$$P[W] = \frac{2e^2 \Omega_1^4 a_1^2 \gamma_\parallel^4}{3c^3} \approx 10^{-42} \left(I \left[\frac{W}{cm^2}\right] \right)^2, \tag{17}$$

for the channeling oscillations amplitude $a_1 \approx 0.1d_{\text{ch}}$. The channel width for the external laser wavelength of $\lambda_0 = 1 \mu m$ crossed at $\eta = 15°$ would be $d_{\text{ch}} \equiv \lambda_0/(2\sin(\eta)) \approx 2\lambda_0 \approx 2 \mu m$.

One should note that, first, both electrons and laser parameters could be chosen so that the radiation wavelength is equal to the external laser one. Hence, this could be interesting as an amplification mechanism for increasing external laser intensity. Moreover, due to rather wide tunable channel width it becomes possible to use a large bunch. In case of, for instance, 10^{10} electrons (monoenergetic, for simplicity), forming a bunch of several μm transverse width, low-frequency *coherent* radiation power is

$$P[W] \approx 10^{-22} \left(I \left[\frac{W}{cm^2}\right] \right)^2. \tag{18}$$

As seen, in the case of initial laser intensity of $10^{17} \text{ W cm}^{-2}$ the total low-frequency radiation power is estimated to be equal to 10^{12} W.

Both of these applications require deep strict analysis of electron beam dynamics taking into account real laser beams parameters. And, obviously, there are some

constraints imposed on channeled electrons. One of them is the bunch divergence. Its critical value could be derived from the channel potential height, and for the parameters above used it can be estimated as ~ 0.1 mrad (it corresponds to the values of $p_\perp/\langle p_\parallel \rangle$ shown in Fig. 3 for over-barrier electrons). In addition, there is an upper limit for the laser intensities to form the channel structure for electrons of particular energies. This is caused by system transition to chaotic behavior described in [39]. The Kapitza method is not applicable for such regimes, which could be observed for different crossing angles as well as laser polarizations. Investigation of such regimes must be done considering electron radiation losses and seems to be very promising for applications as a future new-type γ-radiation source when needed intensities will become achievable (see [40] for details).

IV. SUMMARY

Summing up, channeling of an electron in the field of crossed laser beams was reconsidered with a special attention paid to the peculiarities of the interaction potential. The potential derived in terms of classical physics reveals strong dependence on external lasers parameters and their mutual orientation. Moreover, it shows rather complex dependence on the electron longitudinal velocity by its value and direction. Though the expressions (9) and (10) were reported in [10,31], one may find their derivation, extended analysis, and illustrations presented here interesting.

For the case of p-polarized lasers, the increase in channeled electron longitudinal velocity from $\beta_\parallel \to -1$ (which corresponds to the opposite to Oz-axis electron motion) to β_1^{inv} results in the decrease of the potential amplitude $U_{\mathrm{am}}\gamma_\parallel$ down to zero. In the $[\beta_1^{\mathrm{inv}}; \beta^{\mathrm{min}}]$ interval the potential becomes scattering and grows to its maximum at β^{min}. At the following increase of $\beta_\parallel$ the scattering potential fades away to zero at β_2^{inv}. For $[\beta_2^{\mathrm{inv}}; 1)$ the potential becomes attracting again, growing from zero to its maximum at the end of the interval (this process is shown in [35]). The phenomenon is extensively examined for $\alpha = 0$ in [11–13] and is called "relativistic reversal" in [13]. Nevertheless the analysis for arbitrary α presented above shows that such potential inversion takes place even for completely nonrelativistic electron.

The averaged potential $U_{\mathrm{am}}^c\gamma_\parallel(\alpha, \beta_\parallel)$ for the laser beams of equal circular polarization has exactly the same shape as in the case of p-polarized beams. But its minimal value found at $\beta^{\mathrm{min}} = \sin\alpha^{\mathrm{min}}$ is zero, hence, no potential inversion is observed (the second video in [35]). This fact for counterpropagating circularly polarized lasers was also described in [12,13]. Now it is extended for arbitrary crossing angle.

The radiation spectrum classically calculated is characterized by two major frequencies: the first one is due to

external laser field scattering on relativistic electron, while the second corresponds to the radiation of electron trapped by the effective potential well. The maximum radiation intensity falls on the frequency $\omega_m^{\mathrm{rad}} \sim \gamma_\parallel \sqrt{I}$ defined by both electron energy and external laser intensity, while the integral radiated power depends on squared external laser intensity $P \sim I^2$. Combined with high radiation coherence for a channeled electron bunch it can result in a high intensity gain. The main issue here would be not only electron bunch low-frequency radiation coherency but also electrons cooling due to high-frequency radiation which would be considerable in strong fields.

The expressions for the effective potential and radiation yield were derived mostly for the one-electron case. And the most interesting questions concerning beam dynamics, cooling and coherent radiation in crossed lasers are the subject of our current research that will help to determine the feasibility and conditions for creating tools based on the considered phenomena. We also note that experimental verification of at least potential inversion and reported angular dependence of the effective potential amplitude is possible with currently achievable laser intensities.

[1] P. L. Kapitza and P. A. M. Dirac, Math. Proc. Cambridge Philos. Soc. **29**, 297 (1933).
[2] T. Shintake, Nucl. Instrum. Methods Phys. Res., Sect. A **311**, 453 (1992).
[3] M. V. Fedorov, K. B. Oganesyan, and A. M. Prokhorov, Appl. Phys. Lett. **53**, 353 (1988).
[4] P. Balcou, Eur. Phys. J. D **59**, 525 (2010).
[5] I. A. Andriyash, P. Balcou, and V. T. Tikhonchuk, Eur. Phys. J. D **65**, 533 (2011).
[6] I. A. Andriyash, E. d'Humières, V. T. Tikhonchuk, and P. Balcou, Phys. Rev. Lett. **109**, 244802 (2012).
[7] I. A. Andriyash, E. d'Humières, V. T. Tikhonchuk, and P. Balcou, J. Phys. Conf. Ser. **414**, 012008 (2013).
[8] M. Bertolotti, C. Sibilia, and L. Fuli, in *Trends in Quantum Electronics*, edited by A. M. Prokhorov and I. Ursu (Springer, Berlin Heidelberg, 1986), p. 155.
[9] A. V. Andreev and S. A. Akhmanov, *JETP Lett.* **53**, 18 (1991).
[10] E. N. Frolov, A. V. Dik, and S. B. Dabagov, J. Phys. Conf. Ser. **517**, 012002 (2014).
[11] A. E. Kaplan and A. L. Pokrovsky, Phys. Rev. Lett. **95**, 053601 (2005).
[12] A. L. Pokrovsky and A. E. Kaplan, Phys. Rev. A **72**, 043401 (2005).

[13] P. W. Smorenburg, J. H. M. Kanters, A. Lassise, G. J. H. Brussaard, L. P. J. Kamp, and O. J. Luiten, Phys. Rev. A **83,** 063810 (2011).

[14] J. Lindhard, *Mat.-Fys. Medd.—K. Dan. Vidensk. Selsk.* **34,** 1 (1965).

[15] D. S. Gemmell, Rev. Mod. Phys. **46,** 129 (1974).

[16] M. A. Kumakhov, Phys. Lett. **57A,** 17 (1976).

[17] I. Bukreeva, A. Popov, D. Pelliccia, A. Cedola, S. B. Dabagov, and S. Lagomarsino, Phys. Rev. Lett. **97,** 184801 (2006).

[18] S. B. Dabagov, Phys. Usp. **46,** 1053 (2003).

[19] N. K. Zhevago and V. I. Glebov, Phys. Lett. A **310,** 301 (2003).

[20] V. V. Klimov and V. S. Letokhov, Phys. Lett. A **222,** 424 (1996).

[21] A. Karabarbounis, S. Sarros, and C. Trikalinos, Nucl. Instrum. Methods Phys. Res., Sect. B **316,** 160 (2013).

[22] E. Esarey, B. A. Shadwick, P. Catravas, and W. P. Leemans, Phys. Rev. E **65,** 056505 (2002).

[23] I. Kostyukov, S. Kiselev, and A. Pukhov, Phys. Plasmas **10,** 4818 (2003).

[24] J. Faure, C. Rechatin, O. Lundh, L. Ammoura, and V. Malka, Phys. Plasmas **17,** 083107 (2010).

[25] A. V. Dik, A. Z. Ligidov, and S. B. Dabagov, Nucl. Instrum. Methods Phys. Res., Sect. B **309,** 210 (2013).

[26] E. N. Frolov, A. V. Dik, and S. B. Dabagov, Nucl. Instrum. Methods Phys. Res., Sect. B **309,** 157 (2013).

[27] A. V. Gaponov and M. A. Miller, *J. Exp. Theor. Phys.* **34,** 242 (1958).

[28] B. M. Bolotovskii and A. V. Serov, Phys. Usp. **37,** 515 (1994).

[29] I. A. Andriyash, E. d'Humières, V. T. Tikhonchuk, and P. Balcou, Phys. Rev. ST Accel. Beams **16,** 100703 (2013).

[30] X. Artru, K. A. Ispirian, and M. K. Ispiryan, arXiv:0707.0148.

[31] E. N. Frolov, A. V. Dik, S. B. Dabagov, and K. P. Artyomov, J. Phys. Conf. Ser. **552,** 012035 (2014).

[32] A. F. Elishev, N. A. Filatova, V. M. Golovatyuk *et al.,* Phys. Lett. **88B,** 387 (1979).

[33] L. Fuli, M. Bertolotti, C. Sibilia, C. Ronsivalle, and G. D'Auria, Laser Part. Beams **5,** 557 (1987).

[34] L. D. Landau and E. M. Lifshitz, *Mechanics*, Russian ed. (Nauka, Moscow, 1988).

[35] See Supplemental Material at http://link.aps.org/supplemental/10.1103/PhysRevSTAB.18.064002 for commented video of electron channeling oscillations in electromagnetic lattice.

[36] V. G. Bagrov, V. A. Bordovitsyn, V. Y. Epp *et al., Radiation Theory of Relativistic Particles*, Russian ed. (Fizmatlit, Moscow, 2002), p. 89.

[37] M. A. Kumakhov, R. Wedell *et al., Radiation of Relativistic Light Particles during Interaction with Single Crystals* (Spektrum Akademischer Verlag, Heidelberg-Berlin-New York, 1991).

[38] O. V. Bogdanov, K. B. Korotchenko, and Y. L. Pivovarov, J. Phys. B **41,** 055004 (2008).

[39] D. Bauer, P. Mulser, and W. H. Steeb, Phys. Rev. Lett. **75,** 4622 (1995).

[40] A. Gonoskov, A. Bashinov, I. Gonoskov, C. Harvey, A. Ilderton, A. Kim, M. Marklund, G. Mourou, and A. Sergeev, Phys. Rev. Lett. **113,** 014801 (2014).